Characterization of a Poly(fluorooxetane) and Poly(fluorooxetane-*co*-THF) by MALDI Mass Spectrometry, Size Exclusion Chromatography, and NMR Spectroscopy

Chrys Wesdemiotis,*,† Francesco Pingitore,†,§ Michael J. Polce,† Vernon M. Russell,‡,|| Yongsin Kim,‡ Charles M. Kausch,‡ Thomas H. Connors,‡ Robert E. Medsker,‡,# and Richard R. Thomas*,‡

Department of Chemistry, The University of Akron, Akron, Ohio 44325, and OMNOVA Solutions Inc., 2990 Gilchrist Road, Akron, Ohio 44305-4418

Received May 9, 2006; Revised Manuscript Received September 6, 2006

ABSTRACT: An α,ω-dihydroxypoly(fluorooxetane) was prepared from a fluorinated oxetane monomer and characterized by matrix-assisted laser desorption ionization mass spectrometric (MALDI MS) and gel permeation chromatographic (GPC) methods. Estimated molecular weights were compared to those derived from NMR spectroscopic end-group analysis. The results of 2-D NMR spectroscopic analysis agreed well with 1-D NMR end-group analytical results and MALDI MS experiments. Because of the small molecular weight of the product, the results from the mass spectroscopic and NMR methods compared favorably. The overestimated molecular weights obtained from GPC are explained by aggregation of the amphiphilic poly(fluorooxetane) in a relatively poor solvent. The robustness of the methods was verified by fractionation of the polymer and subsequent analysis of the fractions by MALDI MS. In addition, information regarding product architecture and copolymerization with THF, which was used to complex the BF_3 catalyst, was obtained using tandem mass spectrometry (MS/MS) methods.

Introduction

Poly(oxetanes) are a class of polymers prepared typically by Lewis acid-catalyzed, cationic ring-opening polymerization of oxetane monomers through an activated monomer process.[1−3] The polymerization of oxetane monomers through Lewis acid-catalyzed[4−8] as well as photocationic polymerization[9,10] has been the subject of numerous publications.[11,12]

The present investigation is part of a larger study on the preparation of surface-active poly(fluorooxetane) derivatives. Typically, surfactants are characterized by having a hydrophobe and hydrophile present on the same molecule. The spatial relationship between these functionalities and the overall product architecture can be paramount in determining the optimal size and topology, that will influence surfactant efficiency and free energy of adsorption and can affect product effectiveness. Therefore, structure, architecture, and molecular weight can play a major role in determining effectiveness and efficiency of surface active materials. These important molecular properties are determined here by a combination of chromatographic and multidimensional nuclear magnetic resonance (NMR) and mass spectrometry (MS) methods.

Experimental Section

Materials. The boron trifluoride−tetrahydrofuran (BF_3·THF) complex was purchased from Honeywell, Inc. 3-Methyl-3-[(2,2,2-trifluoroethoxy)methyl]oxetane monomer was prepared as described previously.[13] Neopentyl glycol (Perstorp Polyols), 1,2-dichloroethane (OmniSolve, LC grade; EMD), and methylene chloride (Ashland Chemicals; Technical Grade) were used as received.

Instrumentation. NMR spectroscopy was performed using a Varian Unity 400 spectrometer with probe frequencies of 399.945, 100.575, and 376.282 MHz for ^{1}H, ^{13}C, and ^{19}F observation, respectively. Gel permeation chromatographic results were obtained on a Waters system, fitted with a viscosity (Viscotek model 100) and refractive index detector (Waters model 2414) in 1,2-dichloroethane. Separations were accomplished with three Phenomenex linear high-resolution columns (Phenogel 5 Linear/Mixed; 300 × 7.8 mm) employing a Phenogel 5 Linear/Mixed 50 × 7.8 mm precolumn. The universal calibration curve was generated from a series of narrow dispersity polystyrene standards (Pressure Chemical Co). GPC data were analyzed using Viscotek TriSEC 3.0 GPC software. Universal calibration yielded the Mark−Houwink relationship: $[\eta] = 1.70 \times 10^{-3} M^{0.333}$.

MALDI mass spectra were acquired using a Bruker REFLEX-III time-of-flight (ToF) mass spectrometer (Bruker Daltonics, Billerica, MA). The instrument was equipped with an LSI model VSL-337ND pulsed 337 nm nitrogen laser (3 nm pulse width), a single-stage pulsed extraction ion source, and a two-stage gridless reflector. Mass spectra were obtained in the reflector mode.[14] Solutions of dithranol (20 mg/mL) matrix, polymer (10 mg/mL), and sodium trifluoroacetate (10 mg/mL) were made in tetrahydrofuran (THF). These solutions were mixed in the ratio matrix: cationizing salt:polymer = 2:1:2, and 0.5 μL of the final mixture was deposited on the sample holder. The attenuation of the nitrogen laser was set at 35%.

MALDI tandem mass spectrometry (MS/MS) experiments were conducted on a Waters Q/ToF Ultima quadrupole/orthogonal acceleration ToF mass spectrometer, using the same sample preparation procedure, but with lithium trifluoroacetate as the cationizing agent. The Li^+ adduct of the desired oligomer was mass-selected by the quadrupole and subjected to collisionally activated dissociation (CAD) in a hexapole collision cell. The resulting fragment ions and undissociated oligomer ions were mass-analyzed subsequently by the ToF device.[15] The ions detected in the mass

* To whom correspondence should be addressed. E-mail: wesdemiotis@uakron.edu (C.W.); richard.thomas@omnova.com (R.R.T.).
† The University of Akron.
‡ OMNOVA Solutions Inc.
§ Current address: Department of Chemical Engineering, University of California, Berkeley, CA 94710-2722.
|| Current address: W. L. Gore & Associates, Inc., 555 Papermill Road, Newark, DE 19711.
Current address: EMD Chemicals Inc., 110 EMD Blvd., Savannah, GA 31407.

10.1021/ma0610414 CCC: $33.50
Published on Web 10/26/2006

and CAD tandem mass spectra were singly charged. Hence, mass-to-charge ratios (m/z) and masses (Da) of these ions are identical numerically. The reproducibility of relative abundances was on the order of ±10%.

Synthesis of α,ω-(Dihydroxy)poly(3-methyl-3-[(2,2,2-trifluoroethoxy)methyl]oxetane). A three-necked, 10 L jacketed vessel with heater/chiller bath, thermometer, stir bar, condenser, addition funnel, and inert gas inlet and outlet was charged with dried neopentyl glycol (329.92 g, 3.17 mol), BF_3·THF (177.26 g, 1.27 mol) catalyst, and CH_2Cl_2 (1.86 kg, 21.84 mol) solvent cooled to 25−30 °C. The neopentyl glycol was dried by adding toluene solvent and removing it under reduced pressure. The initiator and catalyst solution was allowed to stir for 30 min at room temperature under a positive pressure nitrogen purge. 3-Methyl-3-[(2,2,2-trifluoroethoxy)methyl]oxetane (3.50 kg, 19.01 mol) was then added to the catalyst/initiator solution at a rate of ∼50 g/min using a pump while maintaining the reaction temperature at 35 ± 10 °C, yielding a monomer-to-catalyst ratio ≈15. The reaction was allowed to stir for 2 h. Additional CH_2Cl_2 was added (2.8 kg, 32.97 mol). Residual BF_3·THF was removed by washing with 2.5 wt % sodium bicarbonate and a water rinse at 40 °C. Solvent was then removed under reduced pressure at 80 °C. α,ω-(Dihydroxy)poly(3-methyl-3-[(2,2,2-trifluoroethoxy)methyl]oxetane) was obtained as a clear, viscous liquid in >95% yield. In addition to the desired polymer, a cyclic tetramer was formed as a byproduct (∼1−5%). The degree of polymerization was determined using ^{1}H NMR spectroscopic end-group analysis and found to be 5.4. The ^{1}H NMR analysis involved prior conversion of the α,ω-dihydroxy groups on the respective polymer to trifluoroacetate derivatives by reaction with trifluoroacetic anhydride. The methylene groups of the α,ω-dihydroxy units have ^{1}H NMR resonances that overlap substantially with the methylene moiety of the pendent fluorinated groups (e.g., $-OCH_2(CF_2)_nF$, $n = 1$) at ∼3.8 ppm. Conversion of the α,ω-dihydroxy groups to trifluoroacetate derivatives shifts the resonance of the adjacent methylene groups downfield to ∼4.3 ppm. The degree of polymerization is calculated by integration of the two methylene signals using the formula degree of polymerization = $2I_{-OCH_2(CF_2)_nF}/I_{-CH_2OC(=O)CF_3}$, where I is the integrated signal of the respective methylene group and the subscripts refer to the pendent fluorinated and terminal trifluoroacetate groups, respectively. It is important to note that polymer chains can be terminated by both initiator (neopentyl glycol) and monomer (oxetane) units. The NMR method sums the two different methylene groups vicinal to the trifluoroacetate terminus. By gel permeation chromatographic analysis, $M_n = 1360$, $M_w = 1990$, and $M_w/M_n = 1.46$. ^{1}H NMR ($CDCl_3$) δ: 0.86−0.95 ($-CH_3$, 3H), 3.20 (backbone$-CH_2-$, 4H), 3.43−3.48 ($-CH_2O-$, 2H), 3.72−3.81 ($-OCH_2-$, 2H). ^{13}C NMR ($CDCl_3$) δ: 17.1−17.3 ($-CH_3$), 41.0−41.4 (backbone$-C-$), 69.0 ($-CH_2-$, q, $J_{^{19}F-^{13}C} = 33.6$ Hz), 75.3−75.5 (backbone$-CH_2-$), 76.0 ($-CH_2O-$), 124.1 ($-CF_3$, q, $J_{^{19}F-^{13}C} = 281$ Hz). For cyclic tetramer, ^{1}H NMR ($CDCl_3$) δ: 0.92 ($-CH_3$, 3H), 3.24−3.14 ($-CH_2-O-CH_2$, m, 4 H), 3.46−3.56 ($-CH_2-O-$, m, 2H), 3.77 ($-O-CH_2-CF_3$, q of t, $J_{^1H-^1H} = 2.2$ Hz, $J_{^{19}F-^1H} = 8.8$ Hz). ^{13}C NMR ($CDCl_3$) δ: 17.36 (s), 41.24 (s), 69.10 (q, $J_{^{19}F-^{13}C} = 33.8$ Hz), 71.73 (s), 76.42 (m), 124.2 (q, $J_{^{19}F-^{13}C} = 280.0$ Hz).

Results and Discussion

Synthesis of Fluorooxetane Monomer and Poly(fluorooxetane) Polymer. The monomer used to prepare the poly(fluorooxetane) required modification of an available hydrocarbon oxetane monomer. The fluorinated oxetane monomer was prepared in high yield by a Williamson ether synthesis using 2,2,2-trifluoroethanol and tetrabutylammonium bromide (TBAB) as phase transfer catalyst (PTC). Details regarding the synthesis of the fluorinated oxetane monomer have been published previously.[13] Polymerization of the fluorinated oxetane monomer was accomplished using neopentyl glycol as initiator and BF_3·THF as a catalyst in CH_2Cl_2 solvent to give a nearly quantitative amount of α,ω-(dihydroxy)poly(3-methyl-3-[(2,2,2-trifluoroethoxy)methyl]oxetane). The polymerization pathway is summarized in Scheme 1. Proton and ^{13}C NMR spectra for the monomer and poly(fluorooxetane) are shown in Figures 1 and 2, respectively. In addition to α,ω-(dihydroxy)poly(3-methyl-3-[(2,2,2-trifluoroethoxy)methyl]oxetane), cyclic oligomers of the oxetane monomer are formed in small (∼5%) yields. The tetramer is the predominant cyclic species and is shown in Scheme 1. The other mers of the cyclic products decrease in abundance by approximately an order of magnitude as the chain length increases beyond tetramer. Proton and ^{13}C NMR spectra for the cyclic tetramer are shown in Figure 3. Furthermore, α,ω-(dihydroxy)poly(3-methyl-3-[(2,2,2-trifluoroethoxy)methyl]oxetane)-*co*-$(THF)_y$ species are produced, with THF monomer arising from catalyst solvent.

Scheme 1. Reaction Scheme for Polymerization of 3-Methyl-3-[(2,2,2-trifluoroethoxy)methyl]oxetane Monomer

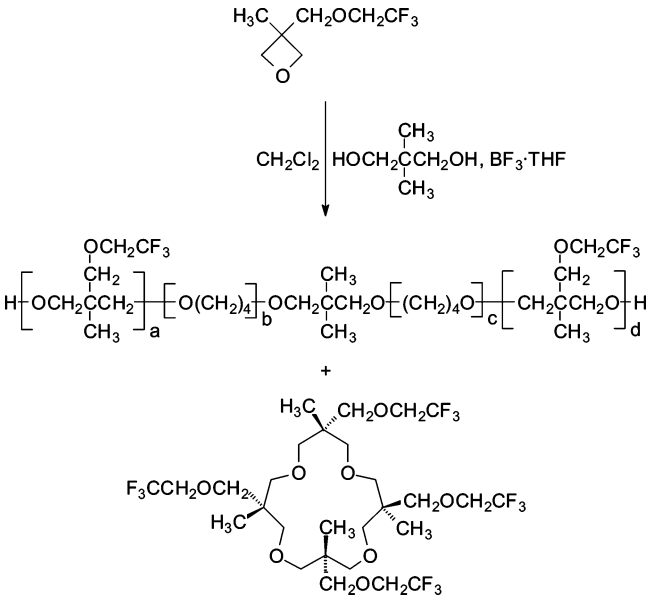

Characterization by NMR. Since the degree of polymerization is low (vide infra), ^{1}H NMR spectroscopy can be used to determine M_n after suitable derivatization of the terminal hydroxyl groups with trifluoroacetic anhydride. For this particular poly(fluorooxetane), NMR end-group analysis yielded a degree of polymerization = 5.4 after removal of the signal contribution due to the cyclic tetramer byproduct. Support for incorporation of THF into the poly(fluorooxetane) is given by the presence of small $-(CH_2)_4O-$ signals at ∼1.6 and ∼3.4 ppm in the ^{1}H NMR spectrum of α,ω-(dihydroxy)poly(3-methyl-3-[(2,2,2-trifluoroethoxy)methyl]oxetane) shown in Figure 1. The high field resonance is hidden beneath the rather complex region at 3−4 ppm. MALDI MS, which can easily distinguish between species of different mass, provides supporting evidence that THF is incorporated into the poly(fluorooxetane) skeleton and is not present as a homopolymer (vide infra).

The differences between an oxetane and neopentyl glycol terminal unit are confirmed from a 2-D NMR (gradient version of the heteronuclear multiple quantum coherence pulse sequence) NMR spectrum shown in Figure 4. Two separate cross-correlated resonances are observed for the terminal methylene groups for the neopentyl glycol (A) initiator and oxetane (B) monomer vicinal to the trifluoroacetate end groups. The ^{1}H end-group resonances were assigned using data from a gradient version of the heteronuclear multiple-bond coherence experiment, showing correlation between the methylene group in $CF_3C(=O)O-CH_2C$ (∼69−73 ppm) and the methylene groups at 4.1 and 4.3 ppm for A and B, respectively.

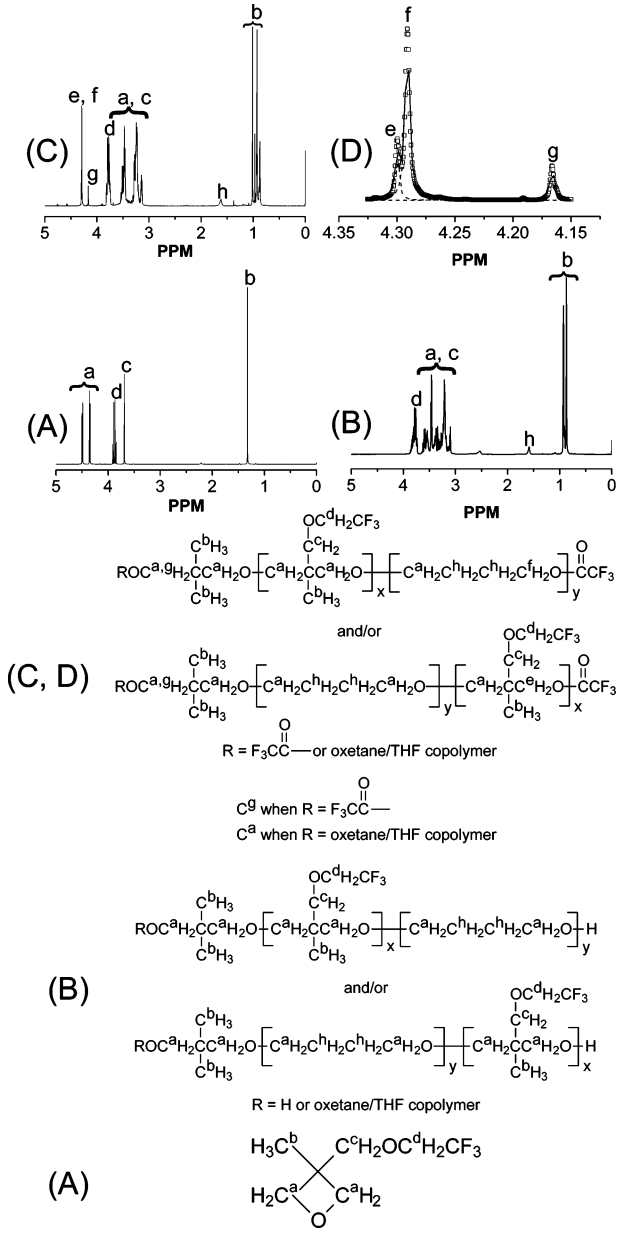

Figure 1. ^{1}H NMR spectra of 3-methyl-3-[(2,2,2-trifluoroethoxy)-methyl]oxetane monomer (A), poly(oxetane) prepared using neopentyl glycol as initiator and BF_3·THF catalyst (B), and trifluoroacetic anhydride-functionalized polymer (C) in $CDCl_3$. Shown in (D) is the expanded terminal region with a Lorentzian curve fit of the three types of terminal functional groups.

Gel Permeation Chromatography. GPC was performed on the poly(fluorooxetane) in 1,2-dichloroethane using universal calibration. The GPC chromatogram is shown in Figure 5. Universal calibration yielded the Mark−Houwink relationship: $[\eta] = 1.70 \times 10^{-3} M^{0.333}$ with $M_n = 1360$, $M_w = 1990$, $M_z = 2780$, and $M_w/M_n = 1.46$. At some small degree of polymerization, the power law dependence of $[\eta]$ with M will change due to the influence of initiator on viscosity. At this point, substantial deviations in molecular weight determined by GPC vs actual will be expected. Currently, the low degree of polymerization limit validity of the Mark−Houwink relationship is unknown.

While NMR studies can provide useful information regarding structure of polymers, they provide neither intimate detail regarding some aspects of architecture nor complete molecular weight analysis such as M_w and polydispersity. This insight can be obtained using GPC and MALDI mass spectroscopic techniques. Typically, GPC is the method of choice for providing information such as M_n, M_w, and, therefore, polydispersity ($= M_w/M_n$). However, the precision and accuracy of GPC for low (<2 kDa) molecular weight polymers (oligomers) are questionable (vide infra) in the current study. GPC also cannot provide connectivity or architectural information. Since surface activity is a strong function of variables such as molecular weight, polydispersity, and architecture, MALDI MS techniques were employed to gain these data. Eventually, the MALDI MS results are compared to NMR end-group analyses and GPC data to provide a more complete structural picture.

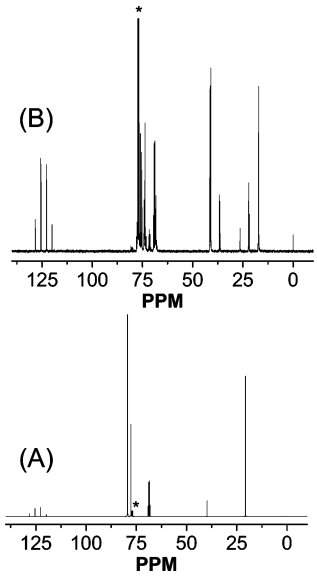

Figure 2. ^{13}C NMR spectrum of 3-methyl-3-[(2,2,2-trifluoroethoxy)-methyl]oxetane monomer (A) and poly(oxetane) prepared using neopentyl glycol as initiator and BF_3·THF catalyst (B) in $CDCl_3$. Peak marked with * is due to $CDCl_3$.

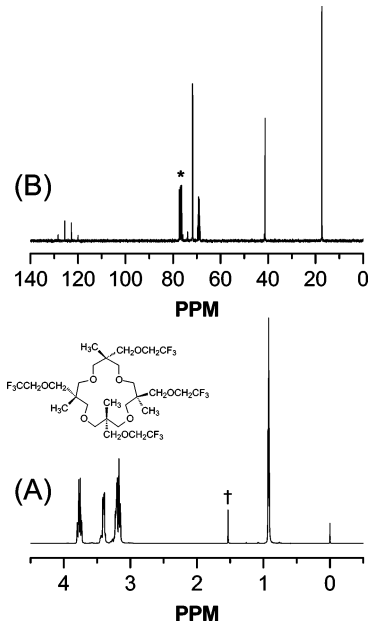

Figure 3. ^{1}H (A) and ^{13}C (B) NMR spectra, in $CDCl_3$, for the cyclic tetramer obtained from polymerization of 3-methyl-3-[(2,2,2-trifluoroethoxy)methyl]oxetane. The resonance denoted by * is due to $CDCl_3$ and † to an impurity.

Compositional Analysis by MALDI Mass Spectrometry. MALDI MS analysis was performed on fractions of the GPC eluent. Starting with an elution volume of 23.5 mL, samples were collected every 30 s for 10 min spanning the transit time

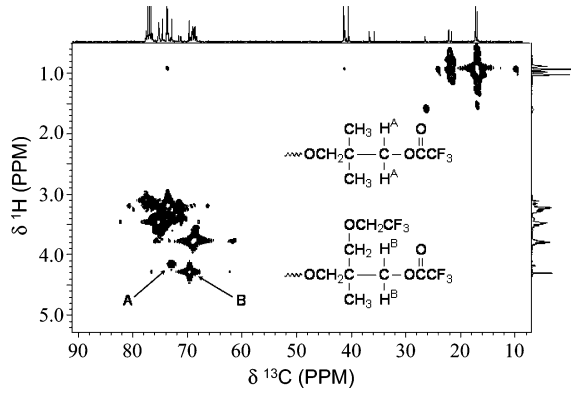

Figure 4. ^{1}H−^{13}C 2-D NMR spectrum of α,ω-(dihydroxy)poly(3-methyl-3-[(2,2,2-trifluoroethoxy)methyl]oxetane) after derivatization with trifluoroacetic anhydride in $CDCl_3$.

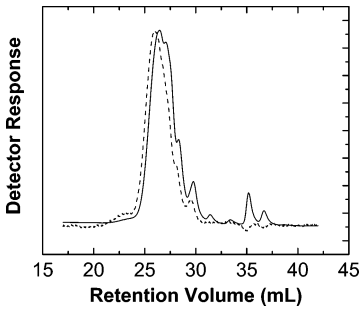

Figure 5. GPC chromatogram for poly(fluorooxetane) in 1,2-dichloroethane. Shown are differential refractometer (—) and viscometric detector responses (- - -).

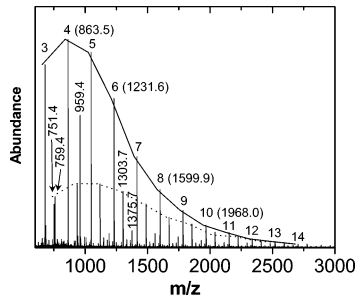

Figure 6. MALDI mass spectrum of unfractionated poly(fluorooxetane) polymer. All ions are Na^+ adducts. Shown are distributions for the poly(fluorooxetane) homopolymer (—) and the poly(fluorooxetane-*co*-$(THF)_1$) (- - -). The numbers 3−14 on top of the homopolymer peaks refer to the degree of polymerization of the oxetane monomer; 2-mers are also observed with low relative abundance (below displayed *m*/*z* range). Select *m*/*z* values are marked above the corresponding oligomer ions. The peak at *m*/*z* 1375.7 belongs to a minor third distribution of poly(fluorooxetane-*co*-$(THF)_2$) copolymer. The peak at 759.4 arises from the cyclic tetramer of the oxetane monomer (see Scheme 1). The peak observed at *m*/*z* 959.4 is due to a contaminant.

of the sample (flow rate = 1.00 mL/min) through the columns under these conditions. The fractionation procedure was repeated identically three times to provide sufficient sample quantities for subsequent analyses.

Because of the relatively "soft" nature of the MALDI method,[16−19] the Na^+ adducts of intact oligomers could be observed using sodium trifluoroacetate as the cationizing agent. Figure 6 shows the MALDI mass spectrum of the native poly(fluorooxetane) sample. Clearly, two different, sizable polymer distributions are exhibited. Isotopically resolved signals are detected for all oligomer ions present in the spectrum. On the basis of the monoisotopic masses measured (i.e., the masses of the all-^{12}C isotopes of the oligomer ions), the most abundant distribution belongs to the poly(fluorooxetane) homopolymer with the generic formula (see Scheme 1): $a + d = 2-14$ and $b + c = 0$. For example, the peak observed at *m*/*z* 1231.6 corresponds to $a + d = 6$: 6 × $C_7H_{11}F_3O_2$ repeat units (6 × 184.071) + $C_5H_{10}O_2$ NPG initiator unit (102.068) + 2 × H end groups (2 × 1.008) + Na^+ (23.000) = 1231.51 (calculated *m*/*z*). A less abundant distribution represents the poly((fluorooxetane)$_{2-14}$-*co*-$(THF)_1$) copolymer where one unit only of THF is incorporated into the polymer backbone: $a + d = 2-14$ and $b + c = 1$. For example, the peak observed at *m*/*z* 1303.7 corresponds to $a + d = 6$ (1231.51, vide supra) plus one ($b + c = 1$) THF unit (72.058) = 1303.57. Just discernible above baseline signal-to-noise are seen ions originating from poly((fluorooxetane)$_{2-14}$-*co*-$(THF)_2$). For example, the peak at *m*/*z* 1375.7 ($a + d = 6$; $b + c = 2$) belongs to this minor distribution. It is important to note that no signals are observed for a homopolymer of THF.

The mass spectrum additionally includes two markedly abundant peaks at *m*/*z* 759 and 959, corresponding to the Na^+ adduct of the cyclic tetramer of the oxetane monomer (see Scheme 1) and an impurity, respectively. The impurity also appeared in blank samples examined with the ToF mass spectrometer but was absent in mass spectra of the native polymer acquired on the Q/ToF mass spectrometer; otherwise, the spectra obtained with the ToF and Q/ToF instruments were quite similar. On the basis of these observations, the impurity is assigned to a contaminant on the sample holder and/or the ion source of the ToF mass spectrometer, originating from samples that contained cyclic tetramer of an oxetane monomer carrying a (pentafluoropropoxy)methyl in place of the (trifluoroethoxy)methyl substituent.

The unfractionated MALDI data were fitted to the standard equations describing molecular weight distributions in polymers (eq 1)[20]

$$M_n = \frac{\sum_i N_i M_i}{\sum_i N_i} \qquad M_w = \frac{\sum_i N_i M_i^2}{\sum_i N_i M_i} \tag{1}$$

where N (given on the ordinate in Figure 6) is the number of molecules having molecular weight M and the index i runs over all oligomer ions (quasi-molecular ions). As can be seen in Figure 6, at least two major distributions are observed: one, in the majority, attributable to the poly(fluorooxetane)$_{2-14}$ homopolymer and the other a poly((fluorooxetane)$_{2-14}$-*co*-$(THF)_1$) copolymer. Standard deviations were calculated using a Monte Carlo simulation (normal distribution) of eq 1 based on a ±10% fluctuation of the relative abundances in the MALDI mass spectra. Reduction of the data for the individual species using eq 1 gave $M_n = 1130 \pm 11$ g/mol, $M_w = 1300 \pm 13$ g/mol, $M_w/M_n = 1.14 \pm 0.02$, and a number-average degree of polymerization ≈ 5.58 for the homopolymer and $M_n = 1330 \pm 13$ g/mol, $M_w = 1490 \pm 14$ g/mol, $M_w/M_n = 1.12 \pm 0.05$, and a number-average degree of polymerization ≈ 6.30 for the copolymer. Analysis of the entire MALDI data set using eq 1 yielded $M_n = 1200 \pm 10$ g/mol, $M_w = 1380 \pm 10$ g/mol, and $M_w/M_n = 1.15 \pm 0.02$. On the basis of integration of the MALDI signals for each species, the molar ratio of poly(fluorooxetane)

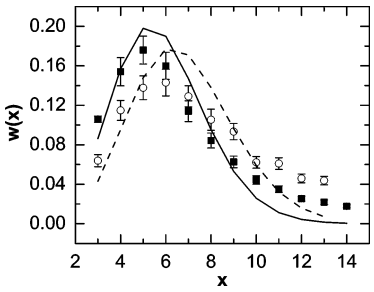

Figure 7. MALDI weight fraction data as a function of the number of monomer units, x, for the poly(fluorooxetane)$_x$ homopolymer (■) and poly((fluorooxetane)$_x$-*co*-(THF)$_1$) copolymer (○). The solid and dashed lines are from a nonlinear least-squares fit of the data to eq 2 for the homopolymer and copolymer, respectively.

homopolymer-to-poly((fluorooxetane)-*co*-(THF)$_1$) copolymer ≈ 0.72/0.28. Given this ratio and the fact that neither free THF was detected in the reaction medium nor was a THF homopolymer formed, it is concluded that THF is incorporated quantitatively into a copolymer with oxetane monomer.

Oligomerization of oxetane monomer (with and without THF) occurs by stepwise growth and the weight fraction of x-mer incorporated into the polymer should follow a Poisson distribution[21,22]

$$w(x) = \left[\frac{x + (M^0 - M)/M}{\nu + M^0/M}\right] e^{-\nu} \nu^{x-1}/(x-1)! \qquad (2)$$

where x is the number of monomer units, M^0 and M are the molecular weights of initiator and monomer, respectively, and ν is the ratio of monomer consumed-to-initiator at time t. As a test of the MALDI technique to provide meaningful data vs theory for step-growth polymerization, MALDI intensity data for the poly(fluorooxetane) homopolymer and poly(fluorooxetane-*co*-(THF)$_1$) copolymer were converted to weight fraction ($w(x) = I_x M_x / \sum_x I_x M_x$ where I is MALDI peak intensity at a given mass, M, with summation over all species x), plotted against x and fitted by nonlinear least-squares analysis using eq 2. For the copolymer case, M^0 was the sum of the molecular weights of initiator and THF. Standard deviations in $w(x)$ were estimated by Monte Carlo simulation (normal distribution) assuming a ±10% variance in MALDI data. The results are shown in Figure 7. The theoretical curve derived from eq 2 captures the salient features of the experimental data considering the errors inherent to the data and calculation of the $w(x)$ term. Fitting yielded $\nu = 4.23 \pm 0.2$, number-average degree of polymerization ≈ 5.23 ± 0.2, $M_n \approx 1100 \pm 40$, $M_w \approx 1200 \pm 50$, and $M_w/M_n \approx 1.09 \pm 0.09$ for the homopolymer and $\nu = 5.27 \pm 0.3$, number-average degree of polymerization ≈ 6.27 ± 0.3, $M_n \approx 1300 \pm 60$, $M_w \approx 1500 \pm 70$, and $M_w/M_n \approx 1.15 \pm 0.1$ for the copolymer, that agree well with the results deduced from the experimental data (vide supra) despite the differences between observed and calculated distribution curves.

Analysis of MALDI intensity data makes the assumption that there are no mass discrimination effects,[17] and the intensity of an individual mer peak gives an accurate account of its true abundance. Both of these assumptions are not, a priori, true necessarily. In general, MALDI MS provides M_n, M_w, and M_w/M_n data that are in very good agreement with analogous data from GPC, if the polymer has low polydispersity ($M_w/M_n < 1.2$). Accurate molecular weights (MW) and molecular weight distributions (MWD) cannot be deduced for polydisperse polymers ($M_w/M_n > 1.4$) via MALDI MS.[16−18] The higher-mass oligomers are discriminated because of lower desorption/ionization, transmission, and detection efficiencies. As a result, M_n and (especially) M_w values deduced from MALDI MS spectra may be significantly lower than those from GPC data, leading to a polydispersity less than the true value. For polymers with M_w/M_n ratios in the 1.2−1.4 range, MALDI mass spectral data sometimes coincide and sometimes disagree with GPC data.

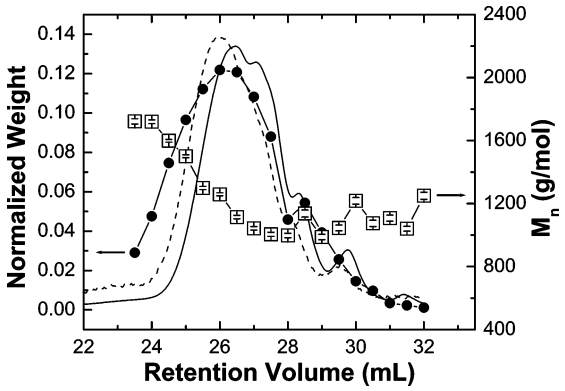

Figure 8. Normalized weight fraction (●) and values of M_n determined from MALDI (□) data for each fraction (poly(fluorooxetane) polymer) superimposed on GPC chromatograph detector response (refractive index (—); viscometric (- - -); arbitrary ordinate).

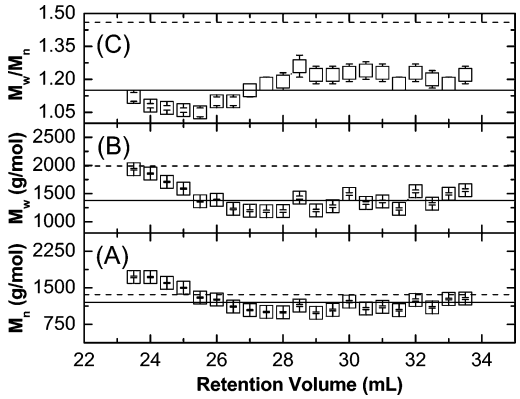

Figure 9. Values of M_n (A), M_w (B), and M_w/M_n (C) determined from MALDI data (poly(fluorooxetane) and poly(fluorooxetane-*co*-THF)) collected on individual fractions along with values determined by MALDI (unfractionated sample) (—) and GPC (- - -).

In an effort to verify the robustness of the MALDI measurements, samples were fractionated during elution through GPC columns, weighed, and then analyzed separately by MALDI MS for comparison. Figure 8 shows the original GPC chromatogram as a function of retention volume along with normalized weight fractions and values of M_n determined by MALDI MS analysis using eq 1 for each fraction. The normalized weights of the fractions matched well the GPC detector responses. The values of M_n determined from MALDI data are for the poly(fluorooxetane) homopolymer distribution only. For a more rigorous characterization, the MALDI fraction data for the poly(fluorooxetane) homopolymer and the poly(fluorooxetane-*co*-THF) copolymer were analyzed according to eq 1. The results of the calculation vs GPC-determined values of M_n, M_w, and M_w/M_n are shown in Figure 9. The agreement between the GPC- and MALDI-determined M_n molecular weight values is satisfactory. Careful examination of the data reveals a larger discrepancy in the values of M_w and as a result M_w/M_n. The poly(fluorooxetane) molecule is surface active in organic solutions. Typical of any surface active agent, it will form micelles or aggregates at a sufficiently high concentration. In organic solutions, these micelles are often small in size and aggregation number.[23] Furthermore, the size and shape of an aggregate and aggregation

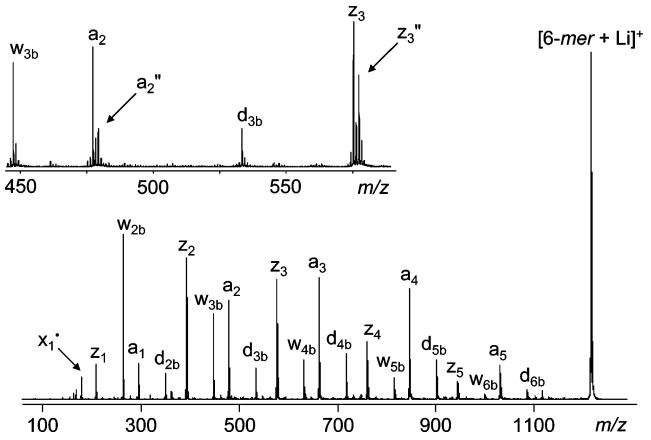

Figure 10. MALDI-CAD tandem mass spectrum of the Li^+ adduct of the poly(fluorooxetane)$_6$ homopolymer. The inset shows an expanded *m*/*z* region in which the six fragment ion series observed are clearly visible (see Table 1 for *m*/*z* values of the fragment ions). The ion marked by $x_1^\bullet$ is the only radical cation detected in the spectrum; it has the connectivity $[^\bullet C(CH_2OCH_2CF_3)(CH_3)CH_2OH + Li]^+$ (*m*/*z* 178).

number are dependent on solvent quality. A Mark−Houwink *a* value of 0.333 indicates that 1,2-dichloroethane, used in GPC measurements, is not a good solvent for the poly(fluorooxetane). A poor solvent would encourage the formation of aggregates. GPC methodology is not able to differentiate a single polymer molecule from an aggregate, thus leading to errors in molecular weight accuracy (higher effective molecular weight) as the extent of aggregation increases.

Sequence Characterization by Tandem Mass Spectrometry. Adding tandem mass spectrometry (MS/MS), i.e., a second dimension of MS analysis, to the MALDI experiment yields additional structural details regarding the architecture of the poly(fluorooxetane). This information is provided by collisionally activated dissociation (CAD) of selected oligomer (quasi-molecular) ions to structure-indicative fragment ions. For the CAD experiments, Li^+ was used to ionize the polymer instead of Na^+, as $[oligomer + Li]^+$ ions yield a larger number of structurally diagnostic fragments, i.e., fragments arising from cleavages along the polymer chain. In contrast, a major dissociation pathway of $[oligomer + Na]^+$ ions is metal ion detachment due to the lower binding affinity of Na^+ vs Li^+ for the polymer. The MALDI-CAD spectrum of the $[6\text{-mer} + Li]^+$ quasi-molecular ion from the poly(fluorooxetane) homopolymer is shown in Figure 10. Three series of fragment ions that differ in end groups are observed and summarized in Table 1. Each series consists of two subsets of fragment ions: one containing the neopentyl glycol (NPG) initiator unit (a_n, a_n'', d_{nb}) and one without (z_n, z_n'', w_{nb}). The six fragment ion series are discerned clearly in the expanded *m*/*z* range displayed in Figure 10. The same types of fragment ions are observed also from the poly(fluorooxetane-*co*-(THF)$_1$) copolymer, as demonstrated by the MALDI-CAD spectrum of the copolymeric $[6\text{-mer} + Li]^+$ ion in Figure 11. Additionally, six further fragment ion distributions appear in this spectrum 72 Da above those formed from the homopolymeric oligomer (Table 2): the latter series arise from fragment ions that contain the THF unit (indicated by T).

The six fragment ion distributions generated from the $[6\text{-mer} + Li]^+$ homopolymer ion have been termed z_n, a_n, z_n'', a_n'', w_{nb}, and d_{nb}, where the subscript "*n*" designates the number of fluorooxetane repeat units in the fragment, while the letter reveals the backbone bond cleaved to yield this fragment and whether it includes the initiator (Scheme 2).[24] The polyoxetane frame contains four types of backbone bonds, whose scissions can potentially generate eight different fragment series: four carrying the initiator unit (a_n, b_n, c_n, d_n) and four without it (w_n, x_n, y_n, z_n). If the NPG initiator were not present, the a_n and z_n series would be indistinguishable, and similarly, $b_n = y_n$, $c_n = x_n$, and $d_n = w_n$. The *m*/*z* values of the observed fragment ion series are consistent with the linear structures shown in Table 1, all of which contain one hydroxy chain end. The other end group is an aldehyde (z_n/a_n), a second hydroxy (z_n''/a_n''), or an alkenyl ether group (w_{nb}/d_{nb}). By convention,[24] fragment ions arising formally via backbone cleavage and subsequent β-H$^\bullet$ loss are designated by a single letter code (e.g., z_n or a_n). If backbone cleavage is succeeded by H$^\bullet$ addition, the single letter code is followed by a double prime (e.g., z_n'' or a_n'') to indicate the 2 Da increase in mass vs fragments formed by H$^\bullet$ loss and having the same number of repeat units. Fragment ions formally arising via backbone cleavage and subsequent β-loss of a side chain are designated by a single letter code followed by a subscript indicative of the lost side chain (e.g., w_{nb} or d_{nb}). The poly(fluorooxetane) studied carries two different side chains on the same C atom, viz. CH_3 (side chain *a*) and $CH_2OCH_2CF_3$ (side chain *b*). Only fragments missing the latter, larger side chain are detected experimentally (Figure 10).

The described nomenclature correlates fragment acronyms to the bonds broken and the end groups created in the CAD process. It does not a priori reveal actual fragmentation mechanisms that must be deduced from the overall fragmentation pattern of the polymer ions. The actual fragments observed in the CAD spectra of Figures 10 and 11 can be reconciled through random homolytic cleavages along the polymer chain with one original end group preserved and creating one new end group. Schemes 3 and 4 provide mechanistic rationalizations that account for the observed fragments.

Polymers ionized by metal ions are known to undergo charge-remote fragmentations when collisionally activated,[25] i.e., the charge is not involved directly in the bond scission process.[26] The weakest bonds in the poly(fluorooxetane) ions investigated should be the C−C bonds at tetrasubstituted C atoms.[27] Cleavage of a $^\bullet CH_2OCH_2CF_3$ radical at such a center gives rise to a relatively stable tertiary radical that can undergo β-C−O bond scission to yield an oxy radical and a terminal alkene held together loosely by the Li^+ cation (cf. Scheme 3).[25] Expulsion of the oxy radical from this complex leads to the w_{nb} and d_{nb} series, as depicted in Scheme 4 (center structure). Alternatively, interligand H$^\bullet$ transfer reactions may take place in the Li^+-bound complex to generate isomeric radical/molecule complexes that subsequently can dissociate to form the fragments of series z_n/a_n (bottom structure) and series z_n''/a_n'' (top structure).

The fluorooxetane monomer and the NPG initiator are similar structurally with both carrying O−C−C(C)$_2$−C connectivities. Comparison of the relative abundances of fragment ion pairs of the same type (e.g., z_n/a_n) and with the same number of O−C−C(C)$_2$−C units shows that the heavier fragments largely contain the initiator, whereas the lighter fragments lack it (cf. Table 1). For example, CH═O-terminated fragments with five O−C−C(C)$_2$−C units (i.e., z_5 and a_4) predominantly carry NPG in their chain ($[a_4]/[z_5] = 6$), while the opposite is true for CH═O-terminated fragments with only two of those units ($[a_1]/[z_2] = 0.3$). These characteristics are consistent with the NPG initiator being incorporated mainly near the center of the polymer chains and the polymer growing from both sides of the initiator, as expected on the basis of molar ratios of reactants used (vide supra).

The fragment ion distributions with common end groups generated from the lithiated 6-mer of poly(fluorooxetane-*co*-(THF)$_1$) can be divided into four categories, depending on

Table 1. Fragment Ions Generated upon CAD of the [6-mer + Li]$^+$ Quasi-Molecular Ion from α,ω-(Dihydroxy)poly(fluorooxetane)[a]

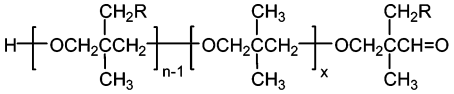

series z_n (x = 0) and a_n (x = 1)

n	z_n (*m/z*)	a_n (*m/z*)	$[a_n] / [z_{n+1}]$[b]
5	943	1029	-
4	759	845	6
3	575	661	2
2	391	477	0.8
1	207	293	0.3

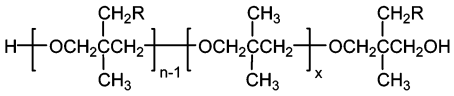

series z_n" (x = 0) and a_n" (x = 1)

n	z_n" (*m/z*)	a_n" (*m/z*)	$[a_n"] / [z_{n+1}"]$[b]
5	945	1031	-
4	761	847	2
3	577	663	1
2	393	479	0.4
1	209	295	0.1

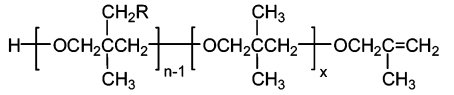

series w_{nb} (x = 0) and d_{nb} (x = 1)

n	w_{nb} (*m/z*)	d_{nb} (*m/z*)	$[d_{nb}] / [w_{(n+1)b}]$[b]
6	999	1085	-
5	815	901	7
4	631	717	2
3	447	533	0.8
2	263	349	0.3
1	-	165	0.03

[a] The fragment ions observed are Li^+ adducts of the oligomers depicted in this table. [b] The ions compared contain the same number of O−C−C(C)$_2$−C units.

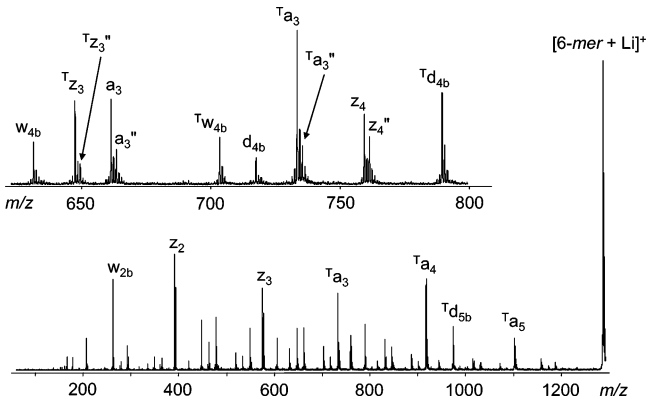

Figure 11. MALDI-CAD mass spectrum in the Li^+ adduct of the poly-((fluorooxetane)$_6$-*co*-(THF)$_1$) copolymer. The inset shows an expanded *m*/*z* region in which the 12 fragment ion series observed are clearly visible (see Table 2 for *m*/*z* values of the fragment ions).

whether they retain or lack the NPG initiator and/or the THF comonomer (cf. Table 2). The fragments of high *m*/*z* value predominantly retain the THF comonomer, while those of low *m*/*z* value have lost it. This trend, observed for the z_n/a_n and z_n''/a_n'', as well as the w_{nb}/d_{nb} series (Table 2), suggests strongly that the THF comonomer is located near the center of the oligomer chains and close to the initiator unit. Such a sequence motif is not surprising considering that the initiator (source of NPG unit) and catalyst (source of THF comonomer) were stirred for 30 min and, therefore, could react with each other before any fluorooxetane monomer was added. Overall, the MS/MS data reveal that the majority of polymer and copolymer chains contain ring-opened fluorooxetane at their chain ends, while the NPG and THF moieties are mainly incorporated into internal positions. A more quantitative evaluation of the end groups is provided by NMR, as will be discussed below.

Each polymer molecule is terminated by hydroxyl groups on both ends that are capable of reacting with trifluoroacetic anhydride. The possible polymer and copolymer end-group configurations are as follows:

$$\begin{gathered} N-O \\ N-T \\ O-N-O \\ T-N-T \\ T-N-O \end{gathered} \qquad (3)$$

where *N*, *O*, and *T* refer to terminal neopentyl, oxetane, and THF groups, respectively. According to these possible configurations, the probabilities, *P*, that a particular end group is present randomly are $P(N) = 0.20$, $P(O) = 0.40$, and $P(T) = 0.40$. However, $[O] = 15[T] = 6[N]$ from reaction stoichiometry, and this will affect the statistics of random end-group termination. Adjusting for the concentration difference and renormalizing

Table 2. Fragment Ions Generated upon CAD of the [6-mer + Li]$^+$ Quasi-Molecular Ion from α,ω-(Dihydroxy)poly(fluorooxetane-*co*-(THF)$_1$)[a]

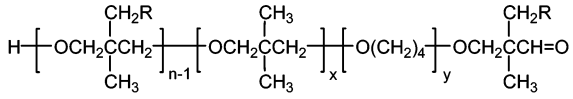

n	z_n (*m/z*)	a_n (*m/z*)	^Tz_n (*m/z*)	^Ta_n (*m/z*)	ratio[b,c]
5	943	1029	1015	1101	-
4	759	845	831	917	3
3	575	661	647	733	1
2	391	477	463	549	0.6
1	207	293	279	365	0.3

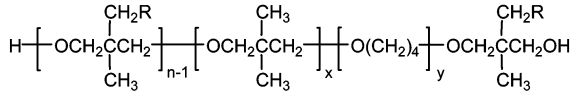

n	z_n" (*m/z*)	a_n" (*m/z*)	^Tz_n" (*m/z*)	^Ta_n" (*m/z*)	ratio[c,d]
5	945	1031	1017	1103	-
4	761	847	833	919	2
3	577	663	649	735	0.8
2	393	479	465	551	0.2
1	209	295	281	367	0.09

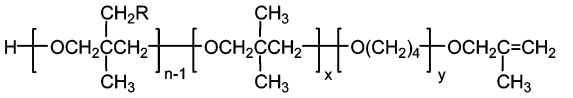

n	w_{nb} (*m/z*)	d_{nb} (*m/z*)	$^Tw_{nb}$ (*m/z*)	$^Td_{nb}$ (*m/z*)	ratio[c,e]
6	999	1085	1071	1157	-
5	815	901	887	973	5
4	631	717	703	789	3
3	447	533	519	605	2
2	263	349	335	421	0.3
1	-	165	-	237	0.06

[a] The fragment ions observed are Li^+ adducts of the oligomers depicted in this table. [b] Ratio = $([^Tz_{n+1}] + [^Ta_n])/([z_{n+1}] + [a_n])$. [c] This ratio compares the abundances of the fragment ions that contain the THF comonomer to the abundances of the fragment ions that have the same number of O−C−C(C)$_2$−C units, but do not contain the THF comonomer. [d] Ratio = $([^Tz_{n+1}''] + [^Ta_n''])/([z_{n+1}''] + [a_n''])$. [e] Ratio = $([^Tw_{(n+1)b}] + [^Td_{nb}])/([w_{(n+1)b}] + [d_{nb}])$.

Scheme 2. Nomenclature for Fragment Ions in the CAD Spectra of Poly(fluorooxetane) Oligomers, Prepared Using Neopentyl Glycol as Initiator[a]

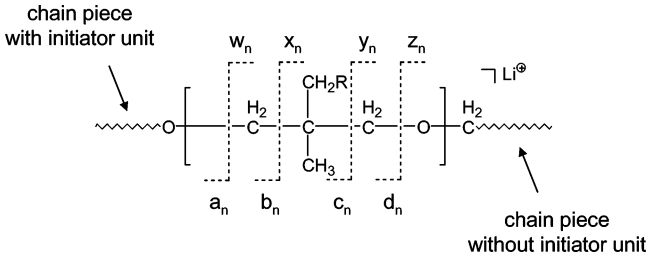

[a] The repeat unit is shown in brackets. R denotes the OCH_2CF_3 group.

the probabilities to the condition $\sum_{i=N}^{T} P_i = 1$ yields $P(N) = 0.13$, $P(O) = 0.81$, and $P(T) = 5.4 \times 10^{-2}$. The integrated ^{1}H NMR data (Figure 1D using a Lorentzian line shape) yields $P(N) = 0.13$, $P(O) = 0.70$, and $P(T) = 0.17$. The discrepancy in the predicted versus observed end-group probabilities is a reflection of the differences in initiation versus propagation rates for the initiator and different monomers. The NMR data are in excellent agreement with the sequence architecture predicted by tandem mass spectrometry: both indicate that the vast majority of polymer chains carry the initiator and comonomer in internal positions, not at the chain ends.

Conclusions

A fluorinated oxetane monomer can be polymerized readily and in high yield using neopentyl glycol as initiator and the boron trifluoride−tetrahydrofuran complex to yield an α,ω-(dihydroxy)poly(fluorooxetane) with low degrees of polymerization. In addition, small (≤∼5%) quantities of cyclic mers are formed with the tetramer dominating. The dihydroxy end groups are amenable to functionalization using trifluoroacetic anhydride. Trifluoroacetate end-group functionalization makes possible the distinguishing of different types of vicinal methylene groups on the poly(oxetane) terminus from those located on interior positions. Integration of the ^{1}H NMR terminal methylene signals can then provide a quantitative measure of the degree of polymerization of the poly(fluorooxetane). Furthermore, trifluoroacetate functionalization provides evidence for the existence of all three possible end groups: neopentyl, oxetane, and tetrahydrofuran. This was substantiated by a 2-D NMR experiment. The source of the tetrahydrofuran incorporated into the poly(fluorooxetane) polymer was from the BF_3·THF complex used as catalyst. While the trifluoroacetate derivatization scheme and ^{1}H NMR end-group analysis provide a degree of polymerization, these data do not provide information sufficient to estimate the other characteristic molecular

Scheme 3. Homolytic Cleavage in a Lithiated Poly(fluorooxetane) Oligomer To Yield a Li^+-Bound Complex between the Emerging Radical/Molecule Species

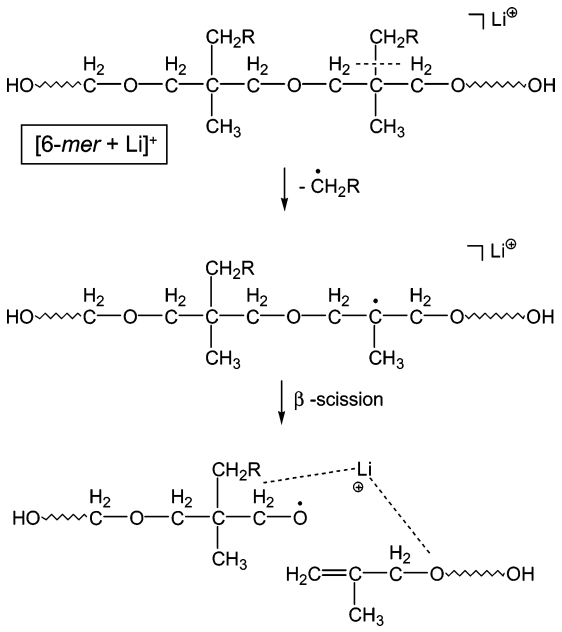

Scheme 4. Isomeric Li^+-Bound Radical/Molecule Complexes Generated via Interligand H Atom Transfers and Their Consecutive Dissociation to the Fragment Ion Series Observed in MS/MS (CAD) Experiments

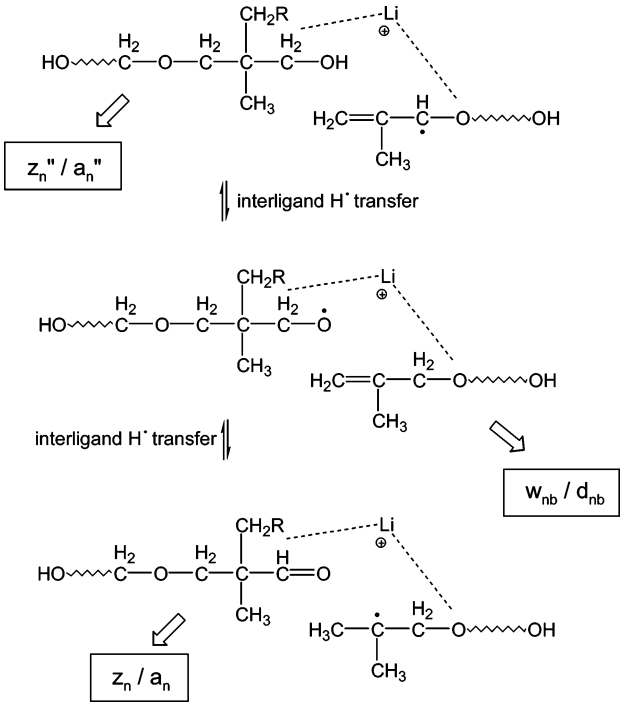

weight values; namely, M_w and M_w/M_n. Estimates of these values were obtained through a combination of GPC chromatographic analysis and MALDI mass spectrometry. Using GPC, M_n = 1360 g/mol, M_w = 1990 g/mol, and M_w/M_n = 1.46. MALDI MS analysis of a native poly(fluorooxetane) sample yielded M_n = 1200 ± 10 g/mol, M_w = 1380 ± 10 g/mol, and M_w/M_n = 1.15 ± 0.02. Analysis of the native MALDI data revealed clearly the presence of a THF copolymer as a minor component with the generic formula poly((fluorooxetane)$_x$-*co*-(THF)$_1$) in addition to a third component of the generic formula poly((fluorooxetane)$_x$-*co*-(THF)$_2$) just visible above background noise. Samples of the poly(fluorooxetane) were fractionated and analyzed individually by MALDI to test for mass discrimination effects. Molecular weight values determined from MALDI analysis of the individual fractions ($M_w/M_n \leq 1.25$) agreed well with the native poly(fluorooxetane) data. The low value of M_w/M_n and its concurrence with that from the native sample substantiate the assumption that mass discrimination effects are not present. The degree of polymerization, estimated by ^{1}H NMR end-group analysis, is ~5.4. For the formula poly((fluorooxetane)$_{5.4}$) $M_n \approx$ 1100 g/mol, and for poly((fluorooxetane)$_{5.4}$-*co*-(THF)$_1$) $M_n \approx$ 1200 g/mol. These values are in excellent agreement with the value of $M_n \approx$ 1200 g/mol obtained from MALDI MS analysis of the native sample. Poly(fluorooxetane) is surface active in solution.[13] This would include the 1,2-dichloroethane solutions used for GPC measurements. Surface activity implies aggregation (micellization) at a sufficiently high concentration. Any aggregation would increase the effective hydrodynamic volume and, subsequently, yield overestimates of the characteristic molecular weight values. Molecular weight parameters characterized by GPC are, indeed, larger than those determined from MALDI or NMR end-group analysis. Tandem MS analysis employing collisionally activated dissociation (CAD) provides evidence that the initiator is incorporated in central positions of the polymer chains and that the THF comonomer is located mainly vicinal to the initiator unit. This structural information was revealed by fragments originating from homolytic cleavage at the fluorinated side chains of the polymer.

Acknowledgment. C.W. thanks the National Science Foundation (CHE-0517909) for generous financial support. This work was also supported by an internship at OMNOVA Solutions Inc. (for F.P.) and by a collaborative grant from OMNOVA Solutions Inc. (to C.W.). The Q/ToF tandem mass spectrometer used in this study was purchased by funds from the Ohio Board of Regents−Hayes Investment Fund Program.

References and Notes

(1) Bednarek, M.; Kubisa, P.; Penczek, S. *Macromolecules* **1999**, *32*, 5257.
(2) Shibasaki, Y.; Sanada, H.; Yokoi, M.; Sanda, F.; Endo, T. *Macromolecules* **2000**, *33*, 4316.
(3) Shibasaki, Y.; Sanda, F.; Endo, T. *Macromolecules* **2000**, *33*, 3590.
(4) Magnusson, H.; Malmström, E.; Hult, A. *Macromolecules* **2001**, *34*, 5786.
(5) Takeuchi, D.; Aida, T. *Macromolecules* **1996**, *29*, 8096.
(6) Bednarek, M.; Kubisa, P.; Penczek, S. *Macromolecules* **2001**, *34*, 5112.
(7) Mai, Y.; Zhou, Y.; Yan, D.; Lu, H. *Macromolecules* **2003**, *36*, 9667.
(8) Kanoh, S.; Nishamura, T.; Ogawa, H.; Motoi, M.; Takani, M. *Macromolecules* **1999**, *32*, 1301.
(9) Thomas, R. R.; Sangermano, M.; Bongiovanni, R.; Malucelli, G.; Priola, A.; Medsker, R. E.; Kim, Y.; Kausch, C. M. *Polymer* **2004**, *45*, 2133.
(10) Sangermano, M.; Malucelli, G.; Bongionvanni, R.; Vescovo, L.; Priola, A.; Thomas, R. R.; Kim, Y.; Kausch, C. M. *Macromol. Mater. Eng.* **2004**, *289*, 722.
(11) Dreyfuss, M. P.; Dreyfuss, P.; Oxetane Polymers. In *Encyclopedia of Polymer Science and Engineering*; Kroschwitz, J., Ed.; Wiley: New York, 1987; Vol. 10, p 653.
(12) Brydson, J. *Plastics Materials*, 2nd ed.; Elsevier: New York, 1999.
(13) Kausch, C. M.; Leising, J. E.; Medsker, R. E.; Russell, V. M.; Thomas, R. R.; Malik, A. A. *Langmuir* **2002**, *18*, 5933.
(14) Arnould, M. A.; Polce, M. J.; Quirk, R. P.; Wesdemiotis, C. *Int. J. Mass Spectrom.* **2004**, *238*, 245.
(15) Wang, P.; Polce, M. J.; Bleiholder, C.; Paizs, B.; Wesdemiotis, C. *Int. J. Mass Spectrom.* **2006**, *249*−*250*, 45.
(16) Nielen, M. W. F.; Malucha, S. *Rapid Commun. Mass Spectrom.* **1997**, *11*, 1194.
(17) Montaudo, G.; Montaudo, M. S.; Samperi, F. Matrix-Assisted Laser Desorption/Ionization. In *Mass Spectrometry of Polymers*; Montaudo, G., Lattimer, R. P., Eds.; CRC Press: Boca Raton, FL, 2002; p 419.

(18) Pasch, H.; Schrepp, W. *Maldi-Tof Mass Spectrometry of Synthetic Polymers*; Springer: Berlin, 2003.
(19) Karas, M.; Hillenkamp, F. *Anal. Chem.* **1988**, *60*, 2299.
(20) Hiemenz, P. C. *Polymer Chemistry the Basic Concepts;* Marcell Dekker: New York, 1984; p 34.
(21) Flory, P. J. *J. Am. Chem. Soc.* **1940**, *62*, 1561.
(22) Billmeyer, F. W., Jr. *Textbook of Polymer Science*, 3rd ed.; Wiley-Interscience: New York, 1984; p 70.
(23) Thomas, R. R.; Glaspey, D. F.; DuBois, D. C.; Kirchner, J. R.; Anton, D. R.; Lloyd, K. G.; Stika, K. M. *Langmuir* **2000**, *16*, 6898.
(24) Jackson, A. T.; Lattimer, R. P.; Price, P. C.; Wallace, W. E.; Polce, M. J.; Wesdemiotis, C. In *Proceedings of the 54th ASMS Conference on Mass Spectrometry and Allied Topics, Seattle, WA, 2006*; Poster No. 5.
(25) Arnould, M. A.; Vargas, R.; Buehner, R. W.; Wesdemiotis, C. *Eur. J. Mass Spectrom.* **2005**, *11*, 243.
(26) Cheng, C.; Gross, M. L. *Mass Spectrom. Rev.* **2000**, *19*, 398.
(27) McMillen, D. G.; Golden, D. M. *Annu. Rev. Phy. Chem.* **1982**, *33*, 493.

MA0610414